

# Global Riemann Solvers for Several $3 \times 3$ Systems of Conservation Laws with Degeneracies

Wen Shen

Mathematics Department, Pennsylvania State University,  
University Park, PA 16802, USA.

March 22, 2022

## Abstract

We study several  $3 \times 3$  systems of conservation laws, arising in modeling of two phase flow with rough porous media and traffic flow with rough road condition. These systems share several features. The systems are of mixed type, with various degeneracies. Some families are linearly degenerate, while others are not genuinely nonlinear. Furthermore, along certain curves in the domain the eigenvalues and eigenvectors of different families coincide. Most interestingly, in some suitable Lagrangian coordinate the systems are partially decoupled, where some unknowns can be solved independently of the others. Finally, in special cases the systems reduce to some  $2 \times 2$  models, which have been studied in the literature. Utilizing the insights gained from these features, we construct global Riemann solvers for all these models. Possible treatments on the Cauchy problems are also discussed.

## 1 Introduction

Scalar conservation laws with discontinuous flux functions have attracted significant research interests in recent years, and exciting progresses have been made. See for example a survey paper [1] and references therein. In a general setting, a scalar conservation law

$$u_t + g(a(x), u)_x = 0 \quad (1.1)$$

where  $a(x)$  contains discontinuity, can be written into a  $2 \times 2$  system, by adding a trivial equation for  $a(x)$ :

$$\begin{cases} u_t + g(a, u)_x = 0, \\ a_t = 0. \end{cases} \quad (1.2)$$

For the general triangular system (1.2), when  $g_u(a, u) = 0$ , the two eigenvalues and eigenvectors of the two families coincide, and the system is not hyperbolic. In the literature this is referred to as parabolic degeneracy. Utilizing the vanishing viscosity solution of

$$\begin{cases} u_t + g(a, u)_x = \varepsilon u_{xx}, \\ a_t = 0, \end{cases} \quad (1.3)$$

as  $\varepsilon \rightarrow 0+$ , solutions of Riemann problems can be uniquely determined. Such admissible condition for jumps in  $a(x)$  leads to the *minimum jump condition*. See [7] and some more recent works [9, 21].

Triangular systems (1.2) arises in many physical models. Take for example the two phase flow models in reservoir simulations. Consider a simple polymer flooding model with single component

$$\begin{cases} s_t + f(s, c)_x = 0, \\ (cs)_t + (cf(s, c))_x = 0. \end{cases} \quad (1.4)$$

Here,  $s \in [0, 1]$  is the saturation of the water phase,  $c \in [0, 1]$  is the fraction of polymer dissolved in water, and  $f(s, c)$  is the fractional flow for the water phase. One assumes uniform porous media, no gravitation force, and no adsorption of the polymer into the porous media. Introducing a Lagrangian coordinate  $(\tau, y)$  (see [25]), with

$$y_x = s, \quad y_t = -f, \quad y(0, 0) = 0, \quad \tau = t,$$

the system (1.4) can be written as a triangular system

$$\begin{cases} (1/s)_\tau - (f(s, c)/s)_y = 0, \\ c_\tau = 0. \end{cases} \quad (1.5)$$

In this paper, we consider the two-phase polymer flooding in rough media, where the permeability function of the porous media may be discontinuous. Let  $k(x)$  be the absolute permeability of the rock, system (1.4) is extended to the following  $3 \times 3$  systems of conservation laws, where we also take into consideration of the adsorption of polymers into the rock:

$$s_t + f(s, c, k)_x = 0, \quad (1.6)$$

$$(m(c) + cs)_t + (cf(s, c, k))_x = 0, \quad (1.7)$$

$$k_t = 0. \quad (1.8)$$

Here, the unknown vector is  $(s, c, k)$ , and the function  $m(c)$  describes the adsorption of polymer in the porous media. We assume that  $m$  depends only on  $c$ .

The main objective of this paper is the construction of global Riemann solvers for (1.6)-(1.8), under 3 different situations:

- We neglect the gravity force and the adsorption. See section 2;
- We consider the adsorption and neglect the gravity force. See section 3;
- We consider the gravity force and neglect the adsorption. See section 5.

As an additional model, we also treat a  $3 \times 3$  system modeling traffic flow in section 4. The traffic flow system has some similar features to the polymer flooding models.

We remark that, global Riemann solvers for general nonlinear systems of hyperbolic conservation laws can not always be constructed, due to the nonlinearity of the flux function. Such a task is possible here, thanks to the special properties of the models. Once a Riemann solver is available, remarks are given on possible approaches to establishing existence of solutions for Cauchy problem, for some of the cases. Finally, concluding remarks are given in section 6 where more future works are suggested.

## 2 A simple model for polymer flooding in two phase flow with rough media

We first consider the two phase flow mode of polymer flooding (1.6)-(1.8), where we neglect the adsorption effect and the gravitation effect, i.e.,

$$s_t + f(s, c, k)_x = 0, \quad (2.1)$$

$$(cs)_t + (cf(s, c, k))_x = 0, \quad (2.2)$$

$$k_t = 0. \quad (2.3)$$

The flux function  $f(s, c, k)$  has the following properties. For any given  $(c, k)$ , the mapping  $s \mapsto f$  is the famous S-shaped Buckley-Leverett function [4] with a single inflection point. We have

$$f(s, c, k) \in [0, 1], \quad f_s(s, c, k) \geq 0, \quad \text{for all } (s, c, k),$$

and

$$f(0, c, k) = 0, \quad f(1, c, k) = 1, \quad f_s(0, c, k) = 0, \quad f_s(1, c, k) = 0, \quad \forall(c, k). \quad (2.4)$$

Furthermore, it's physically reasonable to assume that the flux decreases with more dissolved polymer, and increases with increasing permeability, i.e.,

$$f_c(s, c, k) < 0, \quad f_k(s, c, k) > 0, \quad \forall(s, c, k). \quad (2.5)$$

The assumptions (2.5) simplify the analysis, allowing clearer presentation of the main ideas. We remark that, if we remove the assumptions (2.5), a similar analysis can be carried out, but with heavier details.

## 2.1 Riemann solver for the reduced $2 \times 2$ model

Observe that when  $k$  is constant, the system (2.1)-(2.3) reduces to a  $2 \times 2$  system

$$s_t + f(s, c)_x = 0, \quad (2.6)$$

$$(cs)_t + (cf(s, c))_x = 0. \quad (2.7)$$

With a slight abuse of notation we write  $f(s, c) = f(s, c, k)$  when  $k$  is a constant. The Jacobian matrix of the flux function is triangular

$$J = \begin{pmatrix} f_s(s, c) & f_c(s, c) \\ 0 & f(s, c)/s \end{pmatrix}.$$

The two eigenvalues and the corresponding right eigenvectors of  $J$  are

$$\lambda_s = f_s(s, c), \quad \lambda_c = f(s, c)/s, \quad r_s = \begin{pmatrix} 1 \\ 0 \end{pmatrix}, \quad r_c = \begin{pmatrix} f_c(s, c) \\ \lambda_s - \lambda_c \end{pmatrix}.$$

When  $\lambda_s = \lambda_c$ , the two eigenvectors also coincide, therefore the system becomes parabolic degenerate. Since the difference  $\lambda_s - \lambda_c$  can change sign, nonlinear resonance occurs, and the total variation of the unknown can blow up in finite time, see [22, 23]. Therefore weak solutions  $(s, c)$  are not defined in the class of BV functions.

System (2.6)-(2.7) has been studied in quite some detail in the literature. It is known that Riemann problems for (2.6)-(2.7) can be solved globally, generating entropy solutions that are the vanishing viscosity limit, see [9]. See also a recent work [20], where Riemann problems, as well as the existence of solutions for the Cauchy problems are treated, with the consideration of the gravity force.

We briefly summarize the Riemann solver for (2.6)-(2.7), which will be useful for the solution of the full  $3 \times 3$  system. Given the Riemann data  $(s_l, c_l), (s_r, c_r)$ , we define the functions

$$g(s, c) \doteq f(s, c)/s, \quad g_l(s) \doteq g(s, c_l), \quad g_r(s) \doteq g(s, c_r),$$

and the monotone functions

$$G^\sharp(s; s_r) \doteq \begin{cases} \max \{g_r(s); s \in [s_r, s]\}, & \text{if } s \geq s_r, \\ \min \{g_r(s); s \in [s, s_r]\}, & \text{if } s \leq s_r, \end{cases} \quad (2.8)$$

$$G^\flat(s; s_l) \doteq \begin{cases} \max \{g_l(s); s \in [s_l, s]\}, & \text{if } s \geq s_l, \\ \min \{g_l(s); s \in [s, s_l]\}, & \text{if } s \leq s_l. \end{cases} \quad (2.9)$$

See plots in Figure 1 for illustrations.

Note that the mapping  $s \mapsto G^\sharp$  is increasing, while  $s \mapsto G^\flat$  is decreasing. For any given  $(s_l, s_r)$ , there exists a unique  $\hat{G}$  value where the graphs of the two mappings cross each other. Let  $\sigma$  denote

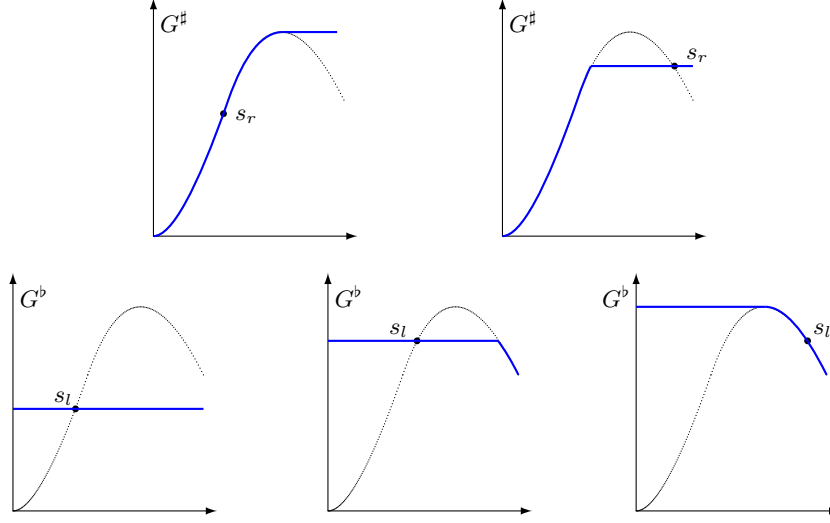


Figure 1: The functions  $G^\sharp(s; s_r)$  and  $G^b(s; s_l)$  for various cases of  $s_r$  and  $s_l$ . The dotted curve is the graph of  $s \mapsto g(s, c)$  for a fixed  $c$ .

the speed of the  $c$  jump, and let  $s_\pm$  denote the traces  $s(t, \sigma t \pm)$  in the Riemann solution. Then,  $s_\pm$  are determined as the *minimum jump path that connects  $G^\sharp$  and  $G^b$* , (see also [7]), where we have

$$g_l(s_-) = G^b(s_-; s_l) = G^\sharp(s_+; s_r) = g_r(s_+) \doteq \sigma. \quad (2.10)$$

Then, the solution of the Riemann problem is obtained by patching together the solution of

$$s_t + f(s, c_l) = 0, \quad s(0, x) = \begin{cases} s_l & (x < 0), \\ s_- & (x > 0), \end{cases} \quad (2.11)$$

for  $x < \sigma t$ , and for  $x > \sigma t$  the solution of

$$s_t + f(s, c_r) = 0, \quad s(0, x) = \begin{cases} s_+ & (x < 0), \\ s_r & (x > 0). \end{cases} \quad (2.12)$$

## 2.2 The Lagrangian coordinate

Define the Lagrangian coordinate  $(\phi, \psi)$  (introduced in [17])

$$\phi_x = -s, \quad \phi_t = f(s, c, k), \quad \phi(0, 0) = 0, \quad \psi = x. \quad (2.13)$$

Here one can interpret  $\phi$  as the potential for the first equation. In fact, for any  $(t, x)$ , the value  $\phi(t, x)$  denotes the line integral

$$\phi(t, x) = \int_{(0,0)}^{(t,x)} f(s, c, k) dt - s dx.$$

Thanks to (2.1), this line integral is path independent. Assuming  $s > 0$  so that  $f > 0$ , the coordinate change is well defined. In this Lagrangian coordinate, the system (2.1)-(2.3) takes the form

$$\left( \frac{1}{f} \right)_\psi - \left( \frac{s}{f} \right)_\phi = 0, \quad (2.14)$$

$$c_\psi = 0, \quad (2.15)$$

$$k_\phi = 0. \quad (2.16)$$

Note that the second and third equations are decoupled. Since  $k$  is a material parameter, the decoupling is not surprising. The decoupling for  $c$  indicates that the thermo-dynamics (governed by (2.15)) is independent of the hydro-dynamics (governed by (2.14)). This is the most interesting feature of the model. It implies that, in the  $(\phi, \psi)$  coordinates,  $k$  is constant along lines parallel to  $\phi$ -axis, and  $c$  is constant along lines parallel to the  $\psi$ -axis.

We illustrate the coordinate change in Figure 2, with Riemann data  $s_l, s_r > 0$ . The line  $t = 0$  now consists of two rays from the origin, in the Lagrangian coordinate  $(\phi, \psi)$ , indicated in blue in Figure 2. For general initial data, the line for  $t = 0$  will be replaced by a curve, continuous and decreasing, but might not be differentiable everywhere. Here we see clearly how the values of  $k$  and  $c$  are “brought into” the region  $t > 0$  from the initial condition.

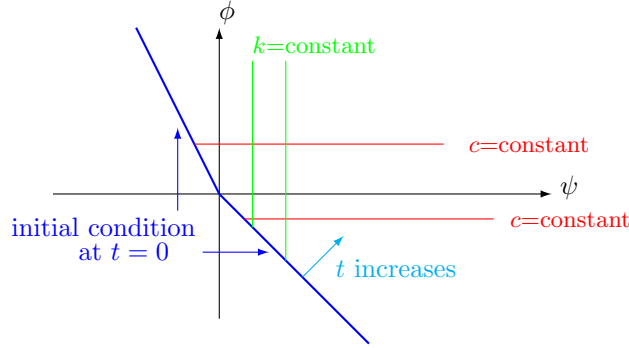


Figure 2: The connection between the two coordinate for Riemann solutions.

Note that when  $s = 0$  then  $f = 0$ , and the conserved quantity for the equation in Lagrangian coordinate blows up to infinity. This is when we have “vacuum”. If  $s(0, x) = 0$  for an intervals  $[x_1, x_2]$ , then the blue curve in Figure 2 will have a horizontal line segment. Since  $c$  has no meaning when  $s = 0$ , we may assign the  $c$  value along this segment as a linear function connecting  $c_1 = c(0, x_1)$  and  $c_2 = c(0, x_2)$ . If  $c_1 \neq c_2$ , then  $c$  has a jump in its solution.

This illustration shows that, once the initial data is given, the values for  $(k, c)$  are known at every point  $(\psi, \phi)$ . In particular, if  $(c, k)$  are initially smooth and  $s(0, x) > 0$ , then  $(c, k)$  remain smooth forever; if they contains discontinuities initially, then they will be discontinuous for  $t > 0$ .

We remark that this Lagrangian coordinate is different from the one used by Wagner in his seminal paper [25], for Euler’s equation. If we apply Wagner’s Lagrangian coordinate to (2.1)-(2.3), only the equation for  $c$  will be decoupled. This doesn’t offer the same insight.

We now consider a scalar conservation law with possibly discontinuous coefficients

$$\left( \frac{1}{f(s; c, k)} \right)_{\psi} - \left( \frac{s}{f(s; c, k)} \right)_{\phi} = 0, \quad (2.17)$$

where  $c, k$  are given functions, possibly discontinuous. A typical plot of the “flux” function, i.e., the graph for the mapping  $(1/f) \mapsto (-s/f)$  is shown in Figure 3.

We remark that scalar conservation laws with horizontal and vertical discontinuities was studied in [5], where Riemann problem and Cauchy problem are studied, under suitable assumption of the flux function. We speculate that an extension of [5] could provide existence and well-posedness for the Lagrangian system (2.14)-(2.16). Details may be worked out in future works. Furthermore, it would also be interesting to obtain equivalent results directly for the Eulerian system, see Remark 2.1.

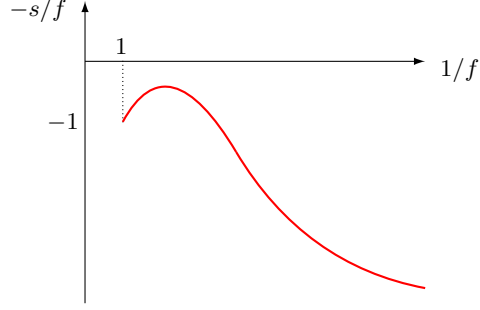


Figure 3: The graph for the mapping  $(1/f) \mapsto (-s/f)$ .

### 2.3 Wave properties and a global Riemann solver

We now return to the full Eulerian system (2.1)-(2.3). Treating  $(s, c, k)$  as the unknown vector, the Jacobian matrix of the flux function is triangular:

$$J = \begin{pmatrix} f_s & f_c & f_k \\ 0 & f/s & 0 \\ 0 & 0 & 0 \end{pmatrix}.$$

Naming the three families as the  $s$ ,  $c$  and  $k$  families, we have the following 3 eigenvalues

$$\lambda_s = f_s, \quad \lambda_c = f/s, \quad \lambda_k = 0,$$

and three corresponding right eigenvectors,

$$r_s = \begin{pmatrix} 1 \\ 0 \\ 0 \end{pmatrix}, \quad r_c = \begin{pmatrix} -f_c \\ f_s - f/s \\ 0 \end{pmatrix}, \quad r_k = \begin{pmatrix} -f_k \\ 0 \\ f_s \end{pmatrix}.$$

Direct computations give:

$$\nabla \lambda_s \cdot r_s = f_{ss}, \quad \nabla \lambda_c \cdot r_c = 0, \quad \nabla \lambda_k \cdot r_k = 0.$$

Thus, the  $c$  and  $k$  families are linearly degenerate, where discontinuities are all contacts, and shock curves coincide with rarefaction curves. For the  $s$  family, since  $f_{ss}$  changes sign, the family is not genuinely nonlinear. However, the integral curves for  $s$  family are straight lines where  $c, k$  are both constants. These integral curves also coincide with the  $s$  shock curves, make it easier to find waves of the  $s$  family. Note also that, when  $f_s = f/s$ , we have  $\lambda_s = \lambda_c$  and  $r_c = r_s$ , and the system is parabolic degenerate, where nonlinear resonance occurs. In summary, the system (2.1)-(2.3) is of Temple class, but of mixed type with degeneracies.

By the Rankine-Hugoniot jump conditions, we have the following wave properties:

- The  $k$  wave is the slowest which travels with speed 0. Along any  $k$  wave, the functions  $f, c$  are continuous;
- The  $c$  wave travels with positive speed. Crossing it,  $f/s, k$  remain continuous;
- The  $s$  wave travels with positive speed. Crossing it,  $c, k$  remain continuous.

Thanks to these wave properties, the solution of the Riemann problem for (2.1)-(2.3) is rather simple. Given the left and right states  $(s_l, c_l, k_l)$  and  $(s_r, c_r, k_r)$ , we have the following global Riemann solver:

- Let  $(s_m, c_l, k_r)$  denote the right state of the  $k$ -wave. The value  $s_m$  is uniquely determined by the condition

$$f(s_m, c_l, k_r) = f(s_l, c_l, k_l).$$

- For the remaining waves, we have  $k \equiv k_r$  throughout. We then solve the Riemann problem for the  $2 \times 2$  system (2.1)-(2.2) with Riemann data  $(s_m, c_l)$  and  $(s_r, c_r)$  as the left and right states. We use the Riemann solver in section 2.1. The solution consists of waves with non-negative speed.

**Remark 2.1.** *It would be of interest to prove existence and well-posedness result for the Cauchy problem directly for the Eulerian system (2.1)-(2.3). The key estimate is the bound on the total wave strength, suitably defined. We expect that the resonance between the  $s$  and  $c$  families can be controlled by Temple-style functionals for wave strength. Then, the total wave strength is non-increasing at interactions between  $s$  and  $c$  waves. However, there are additional difficulties caused by the interactions between  $s$  and  $k$  waves. In strictly hyperbolic cases, this can be controlled by adding a suitable interaction potential functional. However, the interaction potential functional here must take into account the difficulties caused by the vacuum state where  $s = 0$ .*

### 3 Polymer flooding with adsorption in rough media

In this section we consider the polymer flooding with the adsorption effect, but neglect the gravity force:

$$s_t + f(s, c, k)_x = 0, \quad (3.1)$$

$$(m(c) + cs)_t + (cf(s, c, k))_x = 0, \quad (3.2)$$

$$k_t = 0. \quad (3.3)$$

The new term  $m(c)$  denotes the adsorption of polymers into the porous media, which we assume to be a function of  $c$ . Typically one assumes that

$$m'(c) > 0, \quad m''(c) < 0, \quad \forall c.$$

The same coordinate change as (2.13) leads to the following Lagrangian system:

$$\left(\frac{s}{f}\right)_\phi - \left(\frac{1}{f}\right)_\psi = 0, \quad (3.4)$$

$$m(c)_\phi + c_\psi = 0, \quad (3.5)$$

$$k_\phi = 0. \quad (3.6)$$

The equation (3.6) for  $k$  is unchanged. The equation (3.5) for  $c$  is still decoupled, but now  $c$  solves a scalar conservation law, and the  $c$  family is genuinely nonlinear. Nevertheless,  $c$  can be solved independently. Given initial data for  $k, c$ , their values at any point  $(\phi, \psi)$  can be computed first. Then,  $s$  solves the scalar conservation law (2.17) with discontinuous coefficient. The discontinuities include the jumps in  $k$  and shocks in the solution of  $c$ , which has a more complex structure, see Remark 3.1.

#### 3.1 The reduced $2 \times 2$ model

When  $k$  is constant, one has the reduced  $2 \times 2$  system

$$\begin{cases} s_t + f(s, c)_x = 0, \\ (m(c) + cs)_t + (cf(s, c))_x = 0. \end{cases} \quad (3.7)$$

Given Riemann data  $(s_l, c_l), (s_r, c_r)$ , the Riemann problem is studied in the literature, even for multi-component polymers, see [15, 16, 6, 14]. In particular, for any  $(s_l, s_r)$ , if  $c_l > c_r$ , the solution contains a  $c$  shock; and if  $c_l < c_r$  then we have a  $c$  rarefaction.

Consider the case  $c_l > c_r$  where we have a  $c$  shock. We define

$$a \doteq \frac{m(c_l) - m(c_r)}{c_l - c_r}, \quad g_l(s) \doteq \frac{f(s, c_l)}{s + a}, \quad g_r(s) \doteq \frac{f(s, c_r)}{s + a}. \quad (3.8)$$

Define the functions  $G^b, G^\sharp$  as in (2.8)-(2.9), and let  $s_\pm$  be the *minimum jump path* that connects  $G^\sharp$  and  $G^b$ . Then,  $s_\pm$  will be the trace along  $c$  shock which travels with speed

$$\sigma = g_l(s_-) = g_r(s_+).$$

Once the  $c$  shock is located, we patch up the solutions of a regular conservation law on the left and on the right of the  $c$ -shock, as described in section 2.1.

When  $c_l < c_r$  and we have a  $c$  rarefaction wave, the path of the rarefaction wave goes along the integral curves of the  $c$  eigenvectors. See Figure 4 for a typical graph of these integral curves. The resonance point occurs at where the integral curves have horizontal tangent. Thus, the  $c$  rarefaction path must lie either on the left or on the right of the resonance point. Unique path can be chosen to allow feasible solution with increasing wave speeds from left to right. See for example [15]. We omit further details.

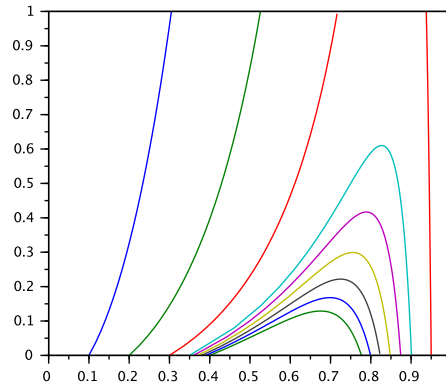


Figure 4: Integral curve for  $c$  family in the  $(s, c)$ -plane.

### 3.2 Wave properties and a global Riemann solver

We go back to the full  $3 \times 3$  system (3.1)-(3.3). The Jacobian matrix for the flux function is again triangular

$$J = \begin{pmatrix} f_s & f_c & f_k \\ 0 & f/(s + m'(c)) & 0 \\ 0 & 0 & 0 \end{pmatrix}$$

with three eigenvalues

$$\lambda_s = f_s(s, c, k), \quad \lambda_c = \frac{f(s, c, k)}{s + m'(c)}, \quad \lambda_k = 0,$$

and three corresponding right-eigenvectors

$$r_s = \begin{pmatrix} 1 \\ 0 \\ 0 \end{pmatrix}, \quad r_c = \begin{pmatrix} -f_c(s, c, k) \\ \lambda_s - \lambda_c \\ 0 \end{pmatrix}, \quad r_k = \begin{pmatrix} -f_k(s, c, k) \\ 0 \\ f_s(s, c, k) \end{pmatrix}.$$



Direct computations give the following directional derivatives:

$$\begin{aligned}\nabla \lambda_s \cdot r_s &= f_{ss}(s, c, k), \\ \nabla \lambda_c \cdot r_c &= \frac{-f(s, c, k)m''(c)(\lambda_s - \lambda_c)}{(s + m'(c))^2}, \\ \nabla \lambda_k \cdot r_k &= 0.\end{aligned}\tag{3.9}$$

We observe the following properties.

- The  $k$  family is linearly degenerate and travels with speed 0, which is the slowest family. Crossing a  $k$  contact, both  $f$  and  $c$  remain continuous.
- The  $c$  family is genuinely nonlinear, as indicated by (3.5) in the Lagrangian system. We can have either a single  $c$  shock or a single  $c$  rarefaction fan in the solution. This fact is not clear from the directional derivatives (3.9) in the Eulerian system. When  $\lambda_s \neq \lambda_c$ , we can rewrite the  $c$  eigenvector as

$$\tilde{r}_c = \begin{pmatrix} \frac{f_c(s, c, k)}{\lambda_c - \lambda_s} \\ 1 \\ 0 \end{pmatrix}.$$

The integral curves for  $\tilde{r}_c$  is now parametrized by  $c$ . Straight computations give

$$\nabla \lambda_c \cdot \tilde{r}_c = -\frac{f(s, c, k)m''(c)}{(s + m'(c))^2} > 0.$$

Therefore, we have a  $c$  rarefaction when  $c_l < c_r$ , and the rarefaction curve can never cross the resonant point where  $\lambda_s = \lambda_c$ . When  $c_l > c_r$ , we have a  $c$  shock.

- The  $s$  family is not genuinely nonlinear, but it's a Temple family where shock curves and rarefaction curves coincide. Crossing a  $s$  wave, both  $c$  and  $k$  remain continuous.

Given any Riemann data  $(s_l, c_l, k_l), (s_r, c_r, k_r)$ , we now have the following global Riemann solver, similar to section 2.3:

- The right state of the  $k$  wave is  $(s_m, c_l, k_r)$  where  $s_m$  is uniquely determined by

$$f(s_l, c_l, k_l) = f(s_m, c_l, k_r).$$

- For the remaining waves, we have  $k \equiv k_r$  which is constant, Then, we solve the Riemann problem for the reduced model (3.7), with left and right states  $(s_m, c_l)$  and  $(s_r, c_r)$  respectively, following the Riemann solver in section 3.1.

**Remark 3.1.** *We remark that wave interaction estimates for this system remain very complicated, and the control of the total wave strength is not available in the literature. In a recent work [10], a scalar conservation law with general discontinuous flux is studied*

$$u_t + f(\alpha(t, x), u)_x = 0, \quad u(0, x) = \bar{u}(x).$$

Here  $\alpha(t, x)$  is discontinuous w.r.t. both variables  $t, x$ . Recall that a function of a single variable  $\alpha : \mathbb{R} \mapsto \mathbb{R}$  is regulated if it admits left and right limits at every point. Such a concept can be extend to functions of two variables. Assuming that  $\alpha(t, x)$  is regulated, in [10] we prove that the vanishing viscosity solutions of

$$u_t + f(\alpha(t, x), u)_x = \varepsilon u_{xx}, \quad u(0, x) = \bar{u}(x)$$

converge to a unique limit solution.

One can show that solutions of scalar conservation laws with convex flux function are regulated functions. An extension of the result in [10] could prove a similar result, at least for the Lagrangian system (3.4)-(3.6). Details may come in future works.

## 4 A second order traffic flow model with rough road condition

As a model of intermediate level of complexity, we consider a  $3 \times 3$  system for traffic flow

$$\rho_t + (\rho v)_x = 0, \quad (4.1)$$

$$[\rho(v + k\rho^\gamma)]_t + [\rho v(v + k\rho^\gamma)]_x = 0, \quad (4.2)$$

$$k_t = 0. \quad (4.3)$$

Here  $\rho \geq 0$  denotes the car density,  $v \geq 0$  is car velocity, and  $k(x) > 0$  denotes the road condition. Furthermore,  $\gamma \in (1, 2)$  is a constant. We consider rough road condition, where  $k(x)$  is discontinuous.

When  $k$  is constant, the reduced system (4.1)-(4.2) was proposed in [2]. Equation (4.1) denotes the conservation of mass. In (4.2), the quantity  $k\rho^\gamma$  denotes some kind of “pressure”. The physical modeling leads to a non-conservative formulation

$$(v + k\rho^\gamma)_t + v \cdot (v + k\rho^\gamma)_x = 0. \quad (4.4)$$

With some algebraic manipulation and utilizing (4.1), one can rewrite (4.4) in the conservative form of (4.2). Although equation (4.2) resembles the conservation of momentum, there is no physical meaning for the conserved quantity  $\rho(v + k\rho^\gamma)$ .

For notational convenience, we denote that

$$w \doteq v + k\rho^\gamma. \quad (4.5)$$

Note that if  $w=\text{constant}$  and  $\rho > 0$ , then (4.2) reduces to (4.1).

### 4.1 A Lagrangian system and the decoupling feature

Consider a Lagrangian coordinate  $(\phi, \psi)$  defined as

$$\phi_x = -\rho, \quad \phi_t = \rho v, \quad \phi(0, 0) = 0, \quad \psi = x.$$

When  $\rho v > 0$ , the coordinate change is well-defined. Direct computation leads to the following Lagrangian system

$$\left(\frac{1}{\rho v}\right)_\psi - \left(\frac{1}{v}\right)_\phi = 0, \quad (4.6)$$

$$w_\psi = 0, \quad (4.7)$$

$$k_\phi = 0. \quad (4.8)$$

We observe the decoupling feature for  $k$  and  $w$  in this Lagrange coordinate. Here  $k$  is constant in  $\phi$ , and  $w$  is constant in  $\psi$ . These features are very similar to those of the system (2.14)-(2.16). Given the initial data at  $t = 0$ , the values of  $(w, k)$  for any coordinate point  $(\phi, \psi)$  are determined trivially, see Figure 2. Once  $(k(\phi, \psi), w(\phi, \psi))$  are given, we can express  $v$  in terms of  $\rho$ , i.e.,

$$v = v(\rho; w, k) = w - k\rho^\gamma. \quad (4.9)$$

Then it remains to solve  $\rho$  using the scalar conservation law (4.6) with variable coefficient,

$$\left(\frac{1}{\rho \cdot (w - k\rho^\gamma)}\right)_\psi - \left(\frac{1}{w - k\rho^\gamma}\right)_\phi = 0, \quad (4.10)$$

where  $(w, k)$  are given functions, possibly discontinuous, and  $\rho$  is the unknown. The discontinuities in the flux function occur along horizontal and vertical lines in the  $(\phi, \psi)$  coordinate.

It would be interesting to explore possible ways of extending the result in [5] for this case, taking extra care of the vacuum state.

## 4.2 Some basic analysis

For the Eulerian system (4.1)-(4.3), treating  $(\rho, v, k)$  as the unknown vector, the Jacobian matrix for the flux function is triangular

$$J = \begin{pmatrix} v & \rho & 0 \\ 0 & v - \gamma k \rho^\gamma & v \rho^\gamma \\ 0 & 0 & 0 \end{pmatrix}.$$

Denoting the three families as the  $\rho$ ,  $v$ , and  $k$  families, we have three eigenvalues

$$\lambda_\rho = v, \quad \lambda_v = v - \gamma k \rho^\gamma, \quad \lambda_k = 0,$$

with three corresponding right-eigenvectors

$$r_\rho = \begin{pmatrix} 1 \\ 0 \\ 0 \end{pmatrix}, \quad r_v = \begin{pmatrix} -1 \\ \gamma k \rho^{\gamma-1} \\ 0 \end{pmatrix}, \quad r_k = \begin{pmatrix} \rho^{\gamma+1} \\ -v \rho^\gamma \\ v - \gamma k \rho^\gamma \end{pmatrix}.$$

Straight computations give

$$\begin{aligned} \nabla \lambda_\rho \cdot r_\rho &= 0, \\ \nabla \lambda_v \cdot r_v &= (\gamma^2 + \gamma) k \rho^{\gamma-1} > 0, \\ \nabla \lambda_k \cdot r_k &= 0. \end{aligned}$$

Thus, the  $\rho$  and  $k$  families are linearly degenerate, where all discontinuities are contacts. The  $v$  family is genuinely nonlinear, where we have either a  $v$  shock or a  $v$  rarefaction in the solution of a Riemann problem. The  $v$  rarefaction curves are integral curves of  $r_v$ .

We consider the  $\rho$  and  $v$  jumps. Observe that crossing both  $\rho$  and  $v$  waves, the value  $k$  remains constant. Fix a  $k$  value, we consider a jump initiated from  $(\rho_0, v_0)$ . Writing  $w_0 = v_0 + k \rho_0^\gamma$ , and letting  $\sigma$  be the jump speed, the RH jump conditions require

$$\sigma(\rho - \rho_0) = \rho v - \rho_0 v_0, \tag{4.11}$$

$$\sigma(\rho w - \rho_0 w_0) = \rho v w - \rho_0 v_0 w_0. \tag{4.12}$$

We first consider the case with vacuum. If  $\rho_0 = 0$ , then for any values of  $v_0$  we have

$$\text{either } \left\{ \rho = 0, \sigma \text{ arbitrary} \right\} \quad \text{or} \quad \left\{ \sigma = v, \rho \text{ arbitrary} \right\}.$$

On the other hand, if  $\rho = 0$ , then for any values of  $v$ , we have

$$\text{either } \left\{ \rho_0 = 0, \sigma \text{ arbitrary} \right\} \quad \text{or} \quad \left\{ \sigma = v, \rho_0 \text{ arbitrary} \right\}.$$

We remark that the vacuum state is special, where the  $v$  and  $\rho$  families have the same eigenvalue and eigenvector, so the system is both parabolic degenerate and linearly degenerate.

For the rest, we assume  $\rho, \rho_0 > 0$ . If  $v = v_0$ , (4.11) gives  $\sigma = v_0 = v$ , and (4.12) trivially holds. This gives a  $\rho$  contact discontinuity. Note that  $\sigma = v_0$  or  $\sigma = v$  leads to the same wave. We conclude that, crossing a  $\rho$  wave, both  $k, v$  remain continuous.

Now we consider the  $v$  shocks, assuming  $v \neq v_0 \neq \sigma$ . Multiplying (4.11) by  $w$  and subtracting from (4.12), we get

$$\rho_0(\sigma - v_0)(w - w_0) = 0.$$

Or symmetrically, multiplying (4.11) by  $w_0$  and subtracting from (4.12), we get

$$\rho(\sigma - v)(w - w_0) = 0.$$

Since  $\rho, \rho_0 > 0$ , this implies

$$w = w_0.$$

The  $v$  shock travels with speed:

$$\sigma_v = \frac{\rho v - \rho_0 v_0}{\rho - \rho_0}.$$

We further observe that, along a  $v$  integral curve,  $w$  remains constant. Indeed, we have

$$\nabla w \cdot r_v = \begin{pmatrix} \gamma k \rho^{\gamma-1} \\ 1 \\ \rho^\gamma \end{pmatrix} \cdot \begin{pmatrix} -1 \\ \gamma k \rho^{\gamma-1} \\ 0 \end{pmatrix} = 0.$$

We conclude that the  $v$  rarefaction curves coincide with  $v$  shock curves. Thus, the  $3 \times 3$  system (4.1)-(4.3) is a Temple class, where the system is of mixed type.

We remark that,

$$\lambda_\rho \geq \lambda_v, \quad \lambda_\rho \geq \lambda_k,$$

but  $\lambda_v - \lambda_k$  may change sign. Thus the possible nonlinear resonance only occurs between the linearly degenerate  $k$  family and the genuinely nonlinear  $v$  family. This fact should make it possible to control the resonance.

We summarize the wave behaviors:

- Crossing a  $k$ -contact, both  $\rho v$  and  $w$  remain continuous.
- Crossing a  $v$ -front,  $w$  and  $k$  remain continuous.
- Crossing a  $\rho$ -contact,  $k$  and  $v$  remain continuous.

Vacuum state is considered as a mixing of  $v$  and  $\rho$  fronts, as it will be clear later. Note also that  $(w, v)$  serve as the natural Riemann invariants for the  $(v, k)$  families, respectively.

### 4.3 The reduced model and its global Riemann solver

When  $k$  is constant, say  $k = 1$ , (4.1)-(4.3) reduces to a  $2 \times 2$  system

$$\begin{cases} \rho_t + (\rho v)_x = 0, \\ [\rho(v + \rho^\gamma)]_t + [\rho v(v + \rho^\gamma)]_x = 0. \end{cases} \quad (4.13)$$

The Riemann problem for (4.13) was studied in much detail in [2]. However, utilizing the Riemann invariants  $(w, v)$ , the Riemann solver can be presented in a very compact manner, as illustrated in Figure 5. Note that the vacuum state  $\rho = 0$  is the straight line  $w = v$  in the  $(w, v)$ -plane, indicated by the red line. The physically feasible region  $\rho \geq 0$  lies on the right side of the vacuum line. Let  $L = (w_l, v_l)$  and  $R = (w_r, v_r)$  be the Riemann data, both lie on the right of the vacuum line. Consider the state  $m = (w_l, v_r)$ . We have two cases:

- If  $m$  lies on the right side of the vacuum line, then the solution of the Riemann problem consists of two waves, with a  $v$ -wave connecting  $L$  to  $m$ , followed by a  $\rho$ -wave connecting  $m$  to  $R$ . The  $v$  wave is a shock if  $v_l > v_r$ , and a rarefaction if  $v_l < v_r$ . See the left plot in Figure 5.
- If  $m$  lies on the left of the vacuum line, then vacuum occurs in the solution, see the right plot in Figure 5. This could only happen when  $v_l < v_r$ . We have two intermediate states  $m_1, m_2$  where  $\rho = 0$ . The solution of the Riemann problem consists of 3 waves: a  $v$  rarefaction connecting  $L$  to  $m_1$ , followed by a vacuum wave connecting  $m_1$  to  $m_2$ , and finally a  $\rho$  contact from  $m_2$  to  $R$ .

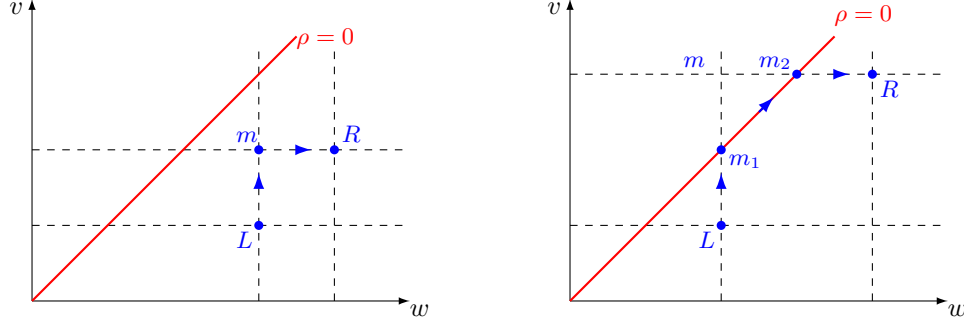


Figure 5: Riemann solver for the  $2 \times 2$  model. Left: Without vacuum, the solution consists of a  $v$ -rarefaction and a  $\rho$ -contact. Right: With an intermediate vacuum wave.

The vacuum wave is rather “fake”, since  $\rho \equiv 0$  is always a solution for any values of  $v$ . To “assign” the  $v$  values along a vacuum wave in the solution of a Riemann problem, we set  $\rho = 0$  in (4.2) and obtain the Burgers’ equation

$$v_t + (v^2/2)_x = 0.$$

Since  $v$  increases from  $m_1$  to  $m_2$ , the solution for  $v$  is a rarefaction wave.

**Continuous dependence.** Viewed in the  $(w, v)$  plane, it is clear that the path for the solution of a Riemann problem depends continuously on the data  $L$  and  $R$ .

**Interaction estimates.** One can define the wave strength as the a Manhattan distance in the  $(w, v)$ -plane, i.e., any wave connecting  $(w_l, v_l)$  and  $(w_r, v_r)$  has the strength

$$|w_l - w_r| + |v_l - v_r|.$$

We claim that the total wave strength remains non-increasing at any interaction. Indeed, we have the following observations:

- Two  $\rho$  waves can not interact with each other since the family is linearly degenerate.
- When a  $\rho$  wave interacts with a  $v$  wave, the total wave strength is unchanged.
- For interactions between two  $v$  waves, the total wave strength is non-increasing since the family is genuinely nonlinear.
- When a vacuum wave interacts with either a  $v$  wave or a  $\rho$  wave, cancellation happens and the total wave strength is decreasing. See Figure 6.

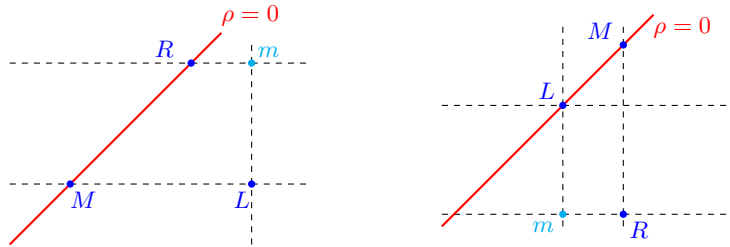


Figure 6: Left: interaction of a vacuum wave with a  $\rho$  wave. Right: interaction of a vacuum wave with a  $v$  wave. Here  $M$  is the middle state of the incoming waves, and  $m$  is the middle state of the outgoing waves.

**Front tracking.** In a front tracking approximation, we approximate  $v$  rarefaction waves with upward jumps of size  $\varepsilon$ . It’s simple to show that the algorithm is well-posed. Total number

of fronts is uniformly bounded. Total wave strength, measured with the Manhattan distance, is also uniformly bounded. Existence of entropy weak solution for the Cauchy problem follows from standard theory.

**Critics for the model.** This second order traffic flow model admits some unreasonable solutions. For example, if  $v(0, x) \equiv 0$ , then  $\rho_t = 0$  and we have the solution  $\rho(t, x) = \rho(0, x)$  for all  $t > 0$ . This means, if cars are initially stationary on a road, they will remain stationary for all time. This unreasonable behavior is caused by the conservation of the “momentum”  $\rho(v + k\rho^\gamma)$ , a concept borrowed from gas dynamics. However, moving cars behave differently from gas particles, and the momentum should not be conserved. High order models for traffic flow are better formulated with a relaxation parameter, where one considers the reaction/acceleration time for each driver.

#### 4.4 Riemann solver for the $3 \times 3$ system

We now describe a global Riemann solver for (4.1)-(4.3). Let  $(\rho_l, v_l, k_l), (\rho_r, v_r, k_r)$  denote the Riemann data, and  $w_l, w_r$  be the correspond  $w$  values. Since the  $\rho$  wave is the fastest one, it will have  $(\rho_r, v_r, k_r)$  as its right state. Denote the left state of the  $\rho$  wave by  $(\rho_m, v_m, k_r)$ . Since  $w$  is constant crossing both  $k$  and  $v$  waves, we have  $w_l$  on the left of the  $\rho$  wave. See Figure 7.

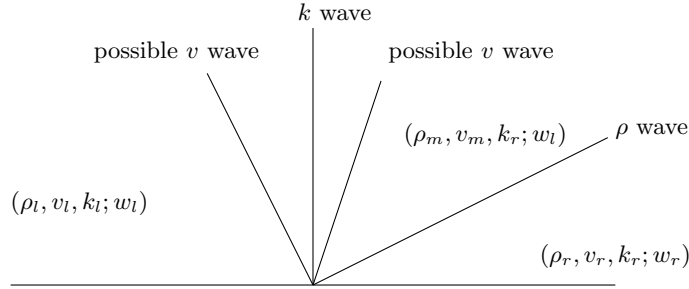


Figure 7: Wave structures in the Riemann solution for the  $3 \times 3$  traffic flow model.

The global Riemann solver consists of two steps.

**Step 1.** We determine the value  $(\rho_m, v_m)$ . There are two cases, with and without the vacuum state.

- If  $w_l \geq v_r$  (see left plot in Figure 8), we can compute the unique value of  $\rho_m$  using

$$v_r + k_r \rho_m^\gamma = w_l.$$

This gives

$$\rho_m = \left( \frac{w_l - v_r}{k_r} \right)^{1/\gamma}, \quad v_m = v_r.$$

- Otherwise if  $w_l < v_r$ , we have a vacuum wave in the solution (see the right plot in Figure 8). From  $m_2$  to  $R$  we have a  $\rho$  wave. On its left there is a vacuum wave that connects  $m_1$  to  $m_2$ . Denote the left state of the vacuum wave as  $(\rho_m, v_m, k_r)$ , we set

$$\rho_m = 0, \quad v_m = w_l.$$

**Step 2.** As the second step, one solves a Riemann problem for the two states

$$(\rho_l, v_l, k_l; w_l), \quad (\rho_m, v_m, k_r; w_l)$$

with only  $k$  wave and  $v$  waves. Since  $w \equiv w_l$  throughout the solution, (4.2) reduces to (4.1). Furthermore, we also have

$$v = v(\rho; k) = w_l - k\rho^\gamma.$$

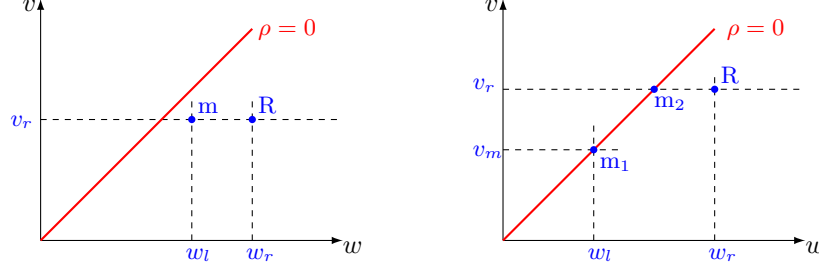


Figure 8: Riemann solver for the  $3 \times 3$  model: The algorithm that determines the  $\rho$ -front. Left: No vacuum. Right: With vacuum and a  $v$ -rarefaction attached on the left of the  $\rho$ -front.

It remains to solve a scalar conservation law with discontinuous flux:

$$\rho_t + (\rho(w_l - k(x)\rho^\gamma))_x = 0, \quad (4.14)$$

where  $k(x)$  is the jump function connecting  $k_l, k_r$  at  $x = 0$ . Calling the flux functions

$$f_l(\rho) = g_l(\rho) = \rho(w_l - k_l\rho^\gamma), \quad f_r(\rho) = g_r(\rho) = \rho(w_l - k_r\rho^\gamma),$$

and defining  $G^\sharp, G^\flat$  accordingly as in (2.8)-(2.9), replacing  $s$  with  $\rho$ . Then, the  $k$  wave is located at the *minimum jump path* that connects  $G^\sharp$  and  $G^\flat$ . The remaining waves in this Riemann solver are determined by patching up solutions, as in (2.11)-(2.12).

In conclusion, we have constructed a global Riemann solver that generates a unique self similar solution for any given left and right state. In the solution, all the quantities  $(\rho, v, k, w)$  are non-negative.

## 5 Polymer flooding with gravity and rough media

We now consider the polymer flooding model (2.1)-(2.3), taking into account the gravitation force but neglect the adsorption effect, i.e.,

$$s_t + f(s, c, k)_x = 0, \quad (5.1)$$

$$(cs)_t + (cf(s, c, k))_x = 0, \quad (5.2)$$

$$k_t = 0. \quad (5.3)$$

An example for the flux function  $f(s, c, k)$  was derived in [8], where the flux function  $f(s, c, k)$  typically becomes negative for small values of  $s$ , see Figure 9. For simplicity of the discussion, we assume the monotone properties (2.4).

### 5.1 Lagrangian coordinates

When we use the Lagrangian coordinate (2.13), it leads to the same system (2.14)-(2.16). Let  $A$  be the Jacobian matrix of the coordinate change, we have

$$A = \begin{pmatrix} f & -s \\ 0 & 1 \end{pmatrix}, \quad \det(A) = f.$$

As  $f$  changes the sign,  $\det(A)$  changes sign as well, reversing the direction of the “time” variable in the Lagrangian system. Since such nonlinear PDE is not time reversible, this coordinate change is not valid.

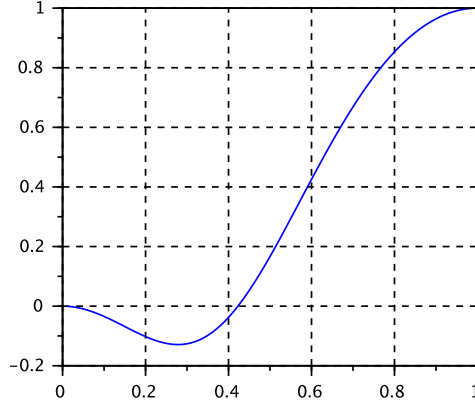


Figure 9: A typical flux function  $s \mapsto f(s, c, k)$  with gravitation force.

In this case, one may introduce a modified Lagrangian coordinate  $(\tilde{\phi}, \tilde{\psi})$  as

$$\tilde{\phi}_x = -\text{sign}(f) \cdot s, \quad \tilde{\phi}_t = \text{sign}(f) \cdot f, \quad \tilde{\phi}(0, 0) = 0, \quad \tilde{\psi} = x. \quad (5.4)$$

This leads to the following Lagrangian system:

$$\begin{cases} \left( \frac{1}{f} \right)_{\tilde{\psi}} - \text{sign}(f) \cdot \left( \frac{s}{f} \right)_{\tilde{\phi}} = 0, \\ c_{\tilde{\psi}} = 0, \\ k_{\tilde{\phi}} = 0. \end{cases} \quad (5.5)$$

## 5.2 The reduced models

There are two types of reduced models, for  $k=\text{constant}$  and for  $c=\text{constant}$ .

**Type 1.** When  $k$  is constant, we have the reduced system (2.6)-(2.7), i.e.,

$$\begin{cases} s_t + f(s, c)_x = 0, \\ (cs)_t + (cf(s, c))_x = 0, \end{cases} \quad (5.6)$$

where  $s \mapsto f$  is as illustrated in Figure 9. The solution of the Riemann problem follows the same Riemann solver as in section 2.1, now with a different flux function  $f(s, c)$ . We remark that, this reduced model was studied in detail in [20], for a more general class of flux function  $f(s, c)$ , where existence of entropy solutions for the Cauchy problem was established.

The solutions of the Riemann problem for (5.6) have the following properties. Let  $(s_l, c_l), (s_r, c_r)$  be the Riemann data, and denote  $f_l = f(s_l, c_l)$ . Let  $s_0 > 0$  be the unique value such that  $f(s_0, c_l) = 0$ . The followings hold.

- If  $s_l < s_0$ , i.e.,  $f_l < 0$ , then the  $c$ -wave in the solution travels with negative speed.
- If  $s_l > s_0$ , i.e.,  $f_l > 0$ , then the  $c$ -wave in the solution travels with positive speed.
- If  $s_l = s_0$ , i.e.  $f_l = 0$ , then the  $c$ -wave is stationary.

We remark that these properties give us the information on the ordering between the  $c$  wave and the  $k$  wave in the Riemann solution of the  $3 \times 3$  system, making that Riemann solver in Section 5.3 easier to construct.



**Type 2.** When  $c \equiv \text{constant}$ , we have the following  $2 \times 2$  system

$$\begin{cases} s_t + f(s, k)_x = 0, \\ k_t = 0. \end{cases} \quad (5.7)$$

Since  $f_s$  can change sign, the system is parabolic degenerate at  $f_s = 0$ . The Riemann solver follows the same construction as for a scalar conservation law with discontinuous flux, where the key step is to locate the path of  $k$  wave. Let  $f_l(s) = f(s, k_l)$  and  $f_r(s) = f(s, k_r)$ , and define  $G^\sharp, G^\flat$  accordingly as in (2.8)-(2.9). The *minimum jump path* connecting  $G^\sharp$  and  $G^\flat$  is the  $k$  wave. The rest follows.

### 5.3 The Riemann solver for the $3 \times 3$ Eulerian system

Regardless of the signs of the wave speeds, we have the following properties:

- The  $k$ -wave travels with speed 0. Crossing it,  $c$  and  $f$  remain continuous;
- Crossing a  $c$ -wave,  $k$  and  $f/s$  remain continuous;
- Crossing an  $s$ -wave,  $k$  and  $c$  remain continuous.

The properties in Section 5.2 give us the sign of the speed for the  $c$  wave, even for the full system. Let  $(s_l, c_l, k_l), (s_r, c_r, k_r)$  be the Riemann data, and let  $f_l = f(s_l, c_l, k_l)$ . Then, if  $f_l < 0$  or  $s_l = 0$ , the  $c$ -wave speed is negative; if  $f_l > 0$ , the  $c$  wave speed is positive. We can now construct the Riemann solver.

**Case (1): The  $c$  wave travels with negative speed.** Let  $(s_m, c_r, k_l)$  denote the trace at  $x = 0-$  in the solution of the Riemann problem. We need to solve two Riemann problems:

(R1): Riemann problem between the states  $(s_l, c_l, k_l)$  and  $(s_m, c_r, k_l)$ , i.e.,

$$\begin{cases} s_t + f(s, c, k_l)_x = 0, \\ (cs)_t + (cf(s, c, k_l))_x = 0, \end{cases} \quad (s, c)(0, x) = \begin{cases} (s_l, c_l), & (x < 0), \\ (s_m, c_r), & (x > 0). \end{cases}$$

This is a reduced model of type 1, discussed in Section 5.2.

(R2): Riemann problem between the states  $(s_m, c_r, k_l)$  and  $(s_r, c_r, k_r)$ , i.e.,

$$\begin{cases} s_t + f(s, c_r, k)_x = 0, \\ k_t = 0, \end{cases} \quad (s, k)(0, x) = \begin{cases} (s_m, k_l), & (x < 0), \\ (s_r, k_r), & (x > 0). \end{cases}$$

This is a reduced model of type 2, discussed in Section 5.2.

For the solution to be plausible, the speeds for the waves of (R1) must be  $< 0$ , and the speeds of the waves of (R2) must be  $\geq 0$ . Here we use the strict “ $<$ ” relation for the waves from (R1), to ensure that  $s_m$  is the trace at  $x = 0-$ , rather than a middle state of two stationary waves.

We denote various related flux functions as:

$$f_l(s) \doteq f(s, c_l, k_l), \quad f_m(s) \doteq f(s, c_r, k_l), \quad f_r(s) \doteq f(s, c_r, k_r).$$

Given the value  $s_l$  and the two flux functions  $f_l, f_m$ , let  $I_1$  denote the set of values for  $s_m$  such that the Riemann problem (R1) is solved with waves of negative speed. Since the Riemann solution for the above system is uniquely defined, the set  $I_1$  can be uniquely constructed, following this general algorithm. For any given  $s_l$ , we locate all possible  $c$  wave paths that travel with negative speed. Then, for all the  $c$  wave paths, we locate all possible  $s_m$  that connects to the  $c$  wave with  $s$  waves of negative speed.

There are 4 cases, illustrated in Figure 11.



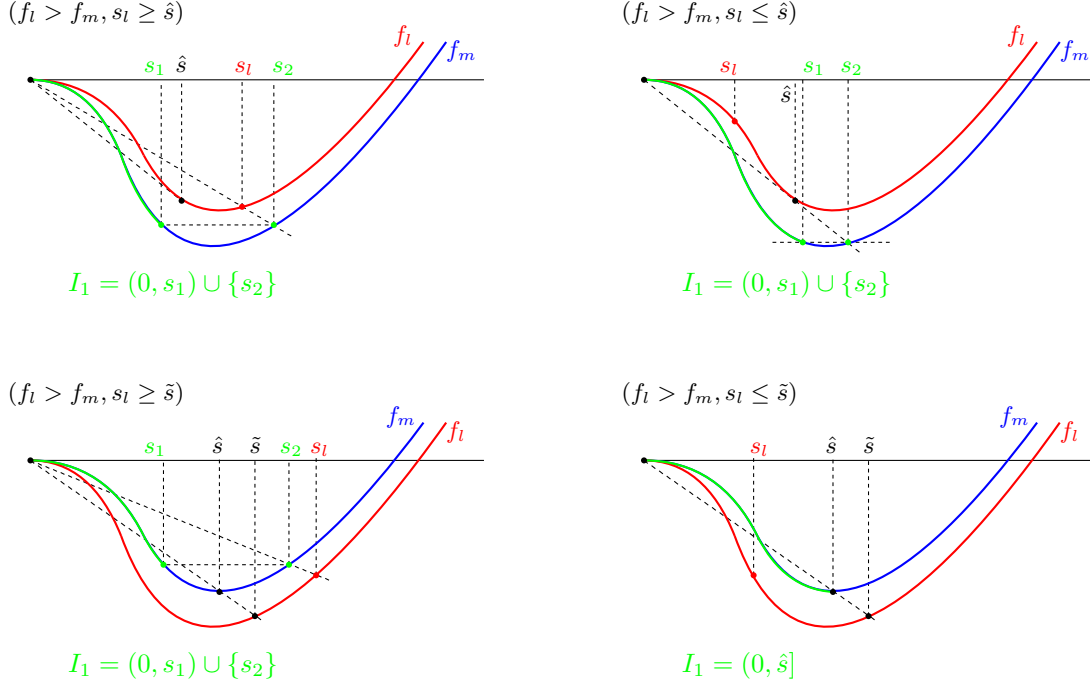


Figure 11: The set  $I_1$  for various cases.

- If  $k_l > k_r$ , we have  $f_m > f_r$ . Let  $\hat{s}$  be the resonant point where  $f'_m(\hat{s}) = 0$ , and  $\tilde{s} < \hat{s}$  satisfies  $f_r(\tilde{s}) = f_m(\hat{s})$ . We have 2 sub-cases.

- For  $s_r \geq \tilde{s}$ , we illustrate it in the top-left plot in Figure 12. Here we simply have

$$I_2 = [\hat{s}, 1].$$

- For  $s_r \leq \tilde{s}$ , we illustrate it in the top-right plot in Figure 12. Here  $s_1 < s_2$  are two unique values such that  $f_m(s_1) = f_m(s_2) = f_r(s_r)$ . The set  $I_2$  contains a closed set  $[s_2, 1]$  and an isolated point  $s_1$ , i.e.,

$$I_2 = [s_2, 1] \cup \{s_1\}.$$

- If  $k_l < k_r$ , we have  $f_m < f_r$ . Let  $\hat{s} > 0$  be the resonant point such that  $f'_r(\hat{s}) = 0$ . Again we have 2 sub-cases.

- The case  $s_r \geq \hat{s}$  is illustrated in the bottom-left plot of Figure 12. Here  $s_1 < s_2$  are chosen such that  $f_m(s_1) = f_r(\hat{s}) = f_m(s_2)$ . We get

$$I_2 = [s_2, 1] \cup \{s_1\}.$$

- The case  $s_r \leq \hat{s}$  is illustrated in the bottom-right plot of Figure 12. Here  $s_1 < s_2$  are chosen such that  $f_m(s_1) = f_r(s_r) = f_m(s_2)$ . We get

$$I_2 = [s_2, 1] \cup \{s_1\}.$$

We now summarize. For all cases, the flux  $f_m$  is decreasing on the set  $I_1$  and increasing on the set  $I_2$ . Furthermore, there exists only one single point on the set  $I_1$  where  $(f_m)' \geq 0$ , and one single point on the set  $I_2$  where  $(f_m)' \leq 0$ . Thus, for any combination of the pair  $I_1, I_2$ , the intersection

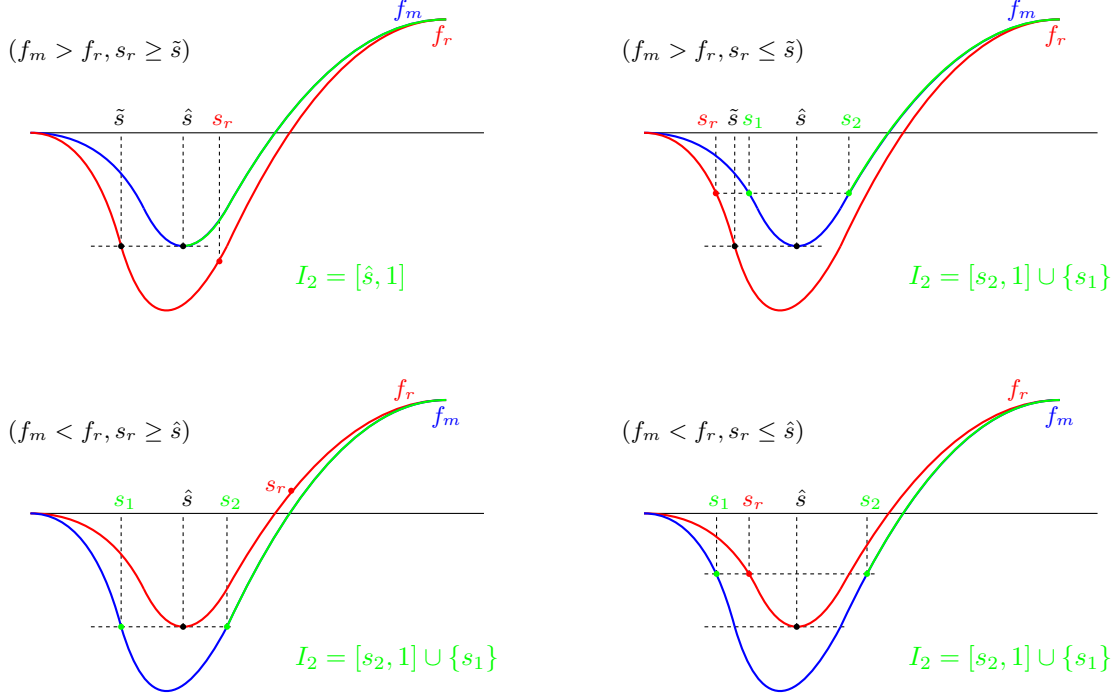


Figure 12: Illustrations for the set  $I_2$  for various cases.

$I_1 \cap I_2$  is non-empty and consists of a exactly one single point. We now let the  $s$  value of this point be the trace  $s_m$ . Note that in all cases, we have  $f_m(s_m) < 0$ .

**Case (2): The  $c$  wave travels with positive speed.** Let  $(s_m, c_l, k_r)$  be the trace along  $x = 0+$ . We have two Riemann problems:

- (R3): Riemann problem connecting states  $(s_l, c_l, k_l)$  and  $(s_m, c_l, k_r)$ , which is a reduced model of type 2, and should be solved with waves of speed  $\leq 0$ .
- (R4): Riemann problem connecting states  $(s_m, c_l, k_r)$  and  $(s_r, c_r, k_r)$ , which is a reduced model of type 1, and should be solved with waves of speed  $> 0$ .

With some abuse of notations, we denote the flux functions

$$f_l(s) \doteq f(s, c_l, k_l), \quad f_m(s) \doteq f(s, c_l, k_r).$$

Let  $I_3$  be the set for the  $s_m$  values such that (R3) is solved with waves of non-positive speed. Recall that  $f_l(s_l) > 0$ . Note then, if  $f_l > 0$  and  $f_m > 0$ , then  $f'_l > 0$  and  $f'_m > 0$ . Thus,  $I_3$  consists of a single point, call it  $s_m$ , such that  $f_l(s_l) = f_m(s_m) > 0$ . As a result, the solution to (R3) consists of a single stationary  $k$ -wave.

It can be easily verified that with this  $s_m$ , Riemann problem (R4) is solved with waves of positive speed.

**Case (3): The  $c$  wave is stationary.** We have  $f(s_l, c_l, k_l) = 0$  and  $s_l > 0$ . Let  $s_m > 0$  be the unique value such that  $f(s_m, c_r, k_r) = 0$ . We have a combined  $c+k$  stationary wave connecting  $(s_l, c_l, k_l)$  to  $(s_m, c_r, k_r)$ . Then,  $(s_m, c_r, k_r)$  can be connected  $(s_r, c_r, k_r)$  by solving a Riemann problem with flux  $f_r(s) = f(s, c_r, k_r)$ . Thanks to the special location of  $s_m$ , the solution consists of waves of non-negative speeds.

In summary, we have a global Riemann solver which generates a unique solution for any initial Riemann data. Furthermore, all discontinuities are entropy admissible, i.e., they are limits of vanishing viscosity solutions of viscous travel waves.

## 6 Concluding Remarks

In this paper we construct global Riemann solvers for several  $3 \times 3$  systems of conservation laws, arising in polymer flooding and traffic flow. However, we neglected the polymer flooding model where both the gravitation force and the adsorptive effect are considered. For system (1.6)-(1.8) where  $s \mapsto f$  is as in Figure 9, the analysis is more complicated, since the Riemann solver for the reduced systems of Type 1 is not available in the literature. Nevertheless, a global Riemann solver can be constructed, following a somewhat similar approach. Due to the new details involved, it deserves to be treated in a separate paper in near future.

It is also interesting to consider the case of multi-component polymer flooding. For the system (1.6)-(1.8), the equation (1.7) is replaced by an  $n \times n$  system, where  $n$  is the number of different types of polymers. The size of the full system is  $(n + 2) \times (n + 2)$ . We denote the families as the  $\{s, c_1, \dots, c_n, k\}$  families. For the non-adsorptive case where  $m(c) = \text{constant}$ , all the  $c_i$  families are linearly degenerate, where all waves travel with non-negative speed and they never interact. A global Riemann solver can be easily constructed in a similar way as the one in Section 2 or Section 4. For the adsorptive model without gravitation force, it depends heavily on the adsorptive function  $m(c)$ , where  $c \in R^n$  and the function  $m(c)$  is vector-valued. In the literature, various adsorptive functions have been studied, leading to very different systems of (1.7). Using the Langmuir isotherm (cf. [19]),

$$m_i(c_1, c_2, \dots, c_n) = \frac{\kappa_i c_i}{1 + \kappa_1 c_1 + \dots + \kappa_n c_n}, \quad i = 1, 2, \dots, n,$$

the systems (1.7) is a Temple class when  $s$  is constant. A rather simple construction for the global Riemann solver can still be achieved following a similar algorithm as in Section 3 and utilizing the reduced Riemann solver in [6].

## References

- [1] B. Andreianov. New approaches to describing admissibility of solutions of scalar conservation laws with discontinuous flux. *ESAIM: Proc. and Surveys*, **50** (2015) pp. 40–65.
- [2] A. Aw and M. Rascle, Resurrection of “Second Order” Models of Traffic Flow. *SIAM J. Appl. Math.*, Vol 60, No. 3, pp. 916–938, (2000).
- [3] P.G. Bedrikovetsky. *Mathematical Theory of Oil and Gas Recovery*. Kluwer Academic Publishers, London, 1993.
- [4] S.E. Buckley, and M. Leverett. Mechanism of fluid displacement in sands. *Transactions of the AIME*, **146** (1942), pp. 107–116.
- [5] Giuseppe Maria Coclite And Nils Henrik Risebro, Conservation Laws With Time Dependent Discontinuous Coefficients. *SIAM J. Math. Anal.* **36** (2005), no. 4, 1293–1309.
- [6] O. Dahl, T. Johansen, A. Tveito, and R. Winther. Multicomponent chromatography in a two phase environment. *SIAM J. Appl. Math.* **52** (1992), pp. 65–104.
- [7] T. Gimse and N. H. Risebro, Riemann problems with a discontinuous flux function. In *Proc. Third Internat. Conf. on Hyperbolic Problems. Theory, Numerical Method and Applications*. (B. Engquist, B. Gustafsson. eds.) Studentlitteratur/Chartwell-Bratt, Lund-Bromley, (1991), pp. 488–502.
- [8] T. Gimse and N. H. Risebro, Solution Of The Cauchy Problem For A Conservation Law With A Discontinuous Flux Function. *SIAM J. Math. Anal.* **23** (1992), pp. 635–648.

- [9] G. Guerra and W. Shen. Vanishing Viscosity Solutions of Riemann Problems for Models in Polymer Flooding. To appear in *Partial Differential Equations, Mathematical Physics, and Stochastic Analysis*, EMS (European Mathematics Society) Series of Congress Reports, a volume in honor of Helge Holden's 60th birthday. Editors: F. Gesztesy, H. Hanche-Olsen, E. Jakobsen, Y. Lyubarskii, N. Risebro, and K. Seip.
- [10] G. Guerra and W. Shen. Vanishing Viscosity Solutions for Conservation Laws with Discontinuous and Regulated Flux. Preprint 2017.
- [11] E. Isaacson, and B. Temple. Analysis of a singular hyperbolic system of conservation laws. *J. Differential Equations*, **65** (1986), pp. 250–268.
- [12] E. Isaacson, and B. Temple. Nonlinear resonance in inhomogeneous systems of conservation laws. *Mathematics of nonlinear science* (Phoenix, AZ, 1989), *Contemp. Math.*, **108**, Amer. Math. Soc., Providence, RI, (1990), pp. 63–77.
- [13] E. Isaacson and B. Temple. Convergence of the  $2 \times 2$  Godunov method for a general resonant nonlinear balance law. *SIAM J. Appl. Math.*, 55(3):625–640, 1995.
- [14] T. Johansen, A. Tveito, and R. Winther. A Riemann solver for a two-phase multicomponent process. *SIAM J. Sci. Statist. Comput.* **10** (1989), pp. 846–879.
- [15] T. Johansen, and R. Winther. The solution of the Riemann problem for a hyperbolic system of conservation laws modelling polymer flooding. *SIAM J. Math. Anal.*, **19** (1988), pp. 541–566.
- [16] T. Johansen and R. Winther. The Riemann problem for multicomponent polymer flooding. *SIAM J. Math. Anal.*, 20(4):908–929, 1989.
- [17] A.P. Pires, P.G. Bedrikovetsky, A.A. Shapiro, A splitting technique for analytical modelling of two-phase multicomponent flow in porous media. *Journal of Petroleum Science and Engineering* **51** (2006), 54–67.
- [18] S. Khorsandi, W. Shen and R.T. Johns. Global Riemann Solver and Front Tracking Approximation of Three-Component Gas Floods. *Quarterly of Applied Mathematics*, Brown University, vol LXXIV, Nr 4, pp. 607-632. (2016).
- [19] H. K. Rhee, R. Aris, and N. R. Amundson. On the theory of multicomponent chromatography. *Philos. Trans. Royal Soc. London*. **267-A** (1970) 419–455.
- [20] W. Shen, On the Cauchy Problems for Polymer Flooding with Gravitation, *J. Differential Equations* **261** (2016) 627–653.
- [21] W. Shen, On the uniqueness of vanishing viscosity solutions for Riemann problems for polymer flooding. To appear in *Nonlinear Differential Equations and Applications NoDEA*, (2017), the Special Issue for 60th Birthday of Alberto Bressan. Guest Editors: F. Ancona, S. Bianchini, A. Marson, P. Marcati.
- [22] B. Temple. Stability and decay in systems of conservation laws. In *Proc. Nonlinear Hyperbolic Problems*, St. Etienne, France, C. Carasso, P. A. Raviart, D. Serre, eds., Springer-Verlag, Berlin, New York, 1986.
- [23] B. Temple. Global solution of the Cauchy problem for a class of  $2 \times 2$  non-strictly hyperbolic conservation laws, *Adv. in Appl. Math.*, **3** (1982), pp. 335–375.
- [24] A. Tveito, and R. Winther. Existence, uniqueness, and continuous dependence for a system of hyperbolic conservation laws modeling polymer flooding. *SIAM J. Math. Anal.* **22** (1991), no. 4, pp. 905–933.
- [25] D. Wagner. Equivalence of the Euler and Lagrangian equations of gas dynamics for weak solutions. *J. Differential Equations*, **68** (1987), pp. 118–136.